

FORWARD NEUTRON CALORIMETER FOR H1 EXPERIMENT AT DESY

A.Bunyatyan^{1,3}, E.Bystritskaya², V.Dodonov^{1,4}, V.Efremenko²,
R.Kutuev^{1,4}, L.Lapin², L.Lytkin^{1,4}, V.Nagovitsin², D.Ozerov²,
B.Povh¹, V.Solochenko^{2,†}, A.Uraev², D.Utkin², A.Zhokin²

¹*Max-Planck-Institut für Kernphysik (Heidelberg),*

²*Institute for Theoretical and Experimental Physics (Moscow),*

³*Yerevan Physics Institute,* ⁴*Joint Institute of Nuclear Research (Dubna),*

[†] *Deceased*

December 5, 2002

Abstract

A new Forward Neutron Calorimeter is designed to measure the energy and the position of high energy neutrons, produced in ep interactions at HERA collider at small angles. The readout of the lead-scintillator sandwich calorimeter is performed by wavelength shifter fibers and photomultipliers. This calorimeter replaces the old spaghetti type calorimeter with deteriorated energy response and was installed during HERA collider luminosity upgrade. The design, construction, tests and calibration with high energy hadron and electron beams are presented in this note.

1 Introduction

The Forward Neutron Calorimeter (FNC) was installed into the H1 experiment in 1996 [1] with purpose to measure the energy and position of highly energetic neutrons produced in reaction $ep \rightarrow enX$ at very small angles (so called leading neutrons). The FNC is located at 107 m from the nominal H1 interaction point so that the final state neutrons with production angles $\theta \lesssim 0.8$ mrad are within the acceptance of the FNC. In 1998, the FNC was upgraded by a preshower calorimeter, which improved the energy and position resolution, and allowed good separation of neutrons from electromagnetic showers (mostly γ -s).

Several physics tasks have been studied with the FNC data, for instance, the triple-differential cross section $d\sigma/(dx dQ^2 dz)$ for the leading neutron production has been measured for the first time at HERA [2], the dijet production in events with leading neutrons is measured in photoproduction and DIS regimes [3].

However, after several years of working (calorimeter was originally used in WA89 experiment at CERN [4]), the response of calorimeter degraded significantly because of radiation damage. The degradation of energy resolution of the FNC ($\sim 20\%$ in the neutron energy range between 300 and 800 GeV) restricted the accuracy of the cross section measurements.

To measure neutrons with adequate precision it was decided, as a part of large H1 upgrade program, to replace the old spaghetti calorimeter with a new tile lead-scintillator sandwich calorimeter read out by the wavelength shifter fibres and the photomultiplier tubes [5]. It was shown in the reference [6] that such calorimeter gives an electron to hadron ratio e/h close to unity, and provides a good hadronic energy resolution $\sigma_E/E = 45\%/\sqrt{E [GeV]}$ with a very small constant term at energies $\leq 70 GeV$. Apart from a good performance, such design allowed to minimize costs and save development and construction time.

2 Design

In this section the design of the Forward Neutron Calorimeter (FNC) is described. The general view of the FNC is shown in Fig.1.

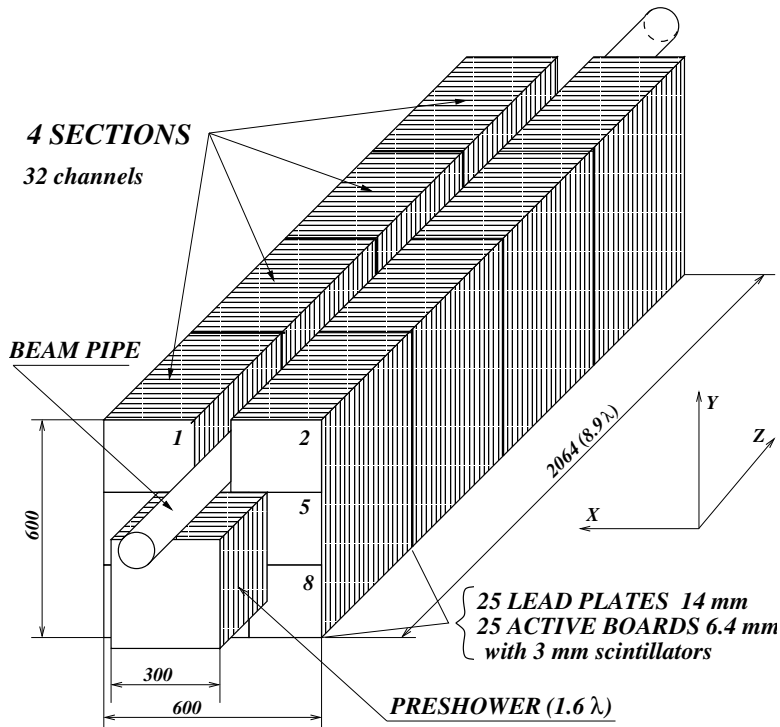


Figure 1: *General view of the installation.*

The FNC consists of the new Main calorimeter and the Preshower. The Preshower was used also in the previous installation and was moved into the new installation without any changes. However, the Preshower is described in this paper as well because its description was never published before.

In addition, two layers of veto counters situated at the distance of 2 m in front of Preshower are used to veto charged particles. Each plane is constructed of 10 mm thick scintillator with transverse size $220 \times 240 \text{ mm}^2$, which fully covers the acceptance region of the calorimeter.

2.1 Preshower

A preshower subdetector was added to a FNC in 1998 in order to improve the energy and position resolution and to provide the separation of neutrons from electromagnetic showers. This is 386 mm ($\sim 1.5\lambda$) long lead–scintillator sandwich calorimeter and it is installed in front of the main calorimeter. The electromagnetic showers completely develop in Preshower, while the hadronic showers leave in Preshower $\sim 40\%$ of their energy (electromagnetic component). So the position resolution for the showers started in Preshower are defined by the electromagnetic component of the shower.

Constructively the Preshower consists of two sections: the electromagnetic and the hadronic ones, each of them is composed of 12 planes. The electromagnetic section is made of thin 2.6 mm scintillators and 7.5 mm lead plates. The hadronic section is made of the double scintillating plates ($2 \times 2.6 \text{ mm}$) and 14 mm lead plates. The transverse size of the scintillating plates is $262 \times 262 \text{ mm}^2$. Each scintillating plate (Fig.2) has 45 grooves with dimension $1.0 \times 0.5 \text{ mm}^2$, where 1.2 mm wavelength shifters (WLS) are glued in. One end of the fibres is coated with aluminium mirror and other going to PM. All fibres have the same length. In order to obtain a good spatial resolution, the orientation of fibres is changed in turn from horizontal to vertical for alternating planes. On each plate the fibres are combined by five into nine strips, longitudinally the strips are combined in 9 vertical and 9 horizontal towers (Fig.3), called x-strips and y-strips afterward in this paper.. The scintillating plates with fibres are wrapped up with *Tyvek* paper and are fixed by spacers in a support between the lead plates. The lead plates lie in the support free and can be easily dismantled.

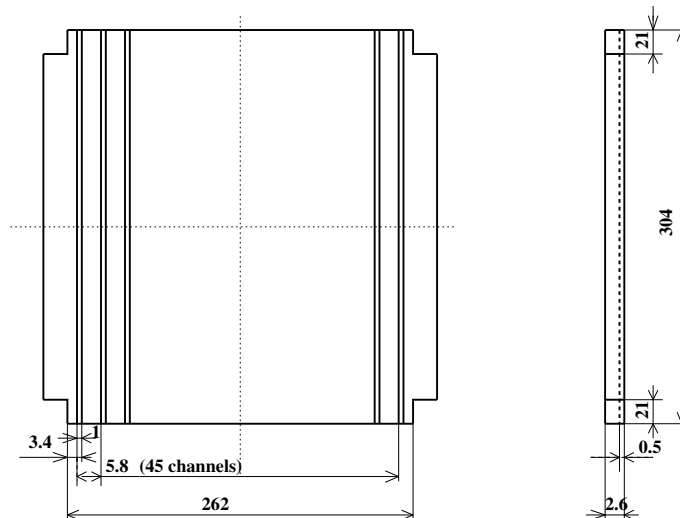


Figure 2: *The Scintillators plate of the Preshower.*

The short-term gain variation of the preshower photomultipliers and light collection by WLS fibres is measured by a LED monitoring system. The light from blue light emitting diodes is coupled by optical fibres to the each strip of one scintilating plate. The average response of the photomultipliers to the LED light is used on a run-by-run basis to correct for small variations in the responses of the photomultipliers which are typically less than one percent and depends on a rate.

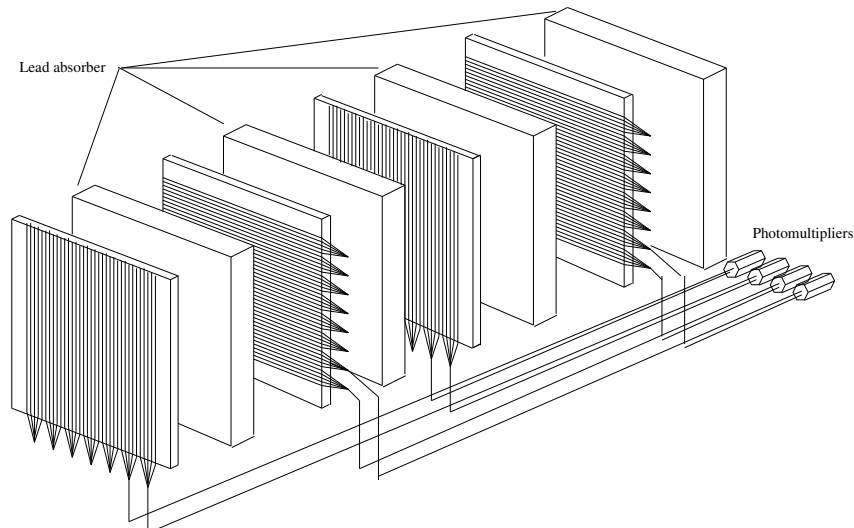


Figure 3: *The scheme of light collection for the Preshower.*

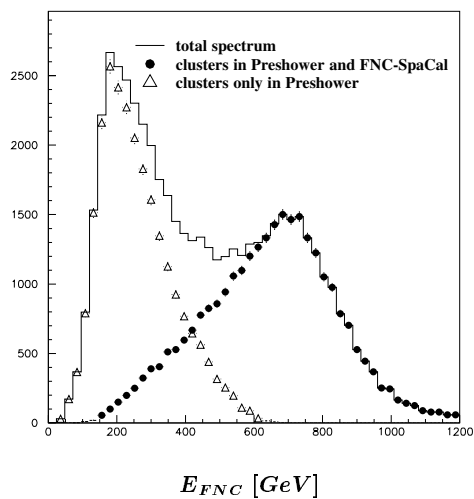


Figure 4: *Energy spectrum of clusters measured by FNC for beam-gas events (1999 data). Distributions are shown separately for clusters contained only in the Preshower (gammas) and clusters which have significant energy deposition in the main spaghetti calorimeter (neutrons).*

The HV settings and preliminary calibration of the Preshower were done with 4 GeV electron beam at DESY beam test facility in 1998. The energy resolution for electromagnetic showers is $\sim 20\%/\sqrt{E}$ [GeV] and the spatial resolution is ~ 2 mm.

Apart from improvement the energy and position resolution the Preshower provides efficient separation of electromagnetic and hadronic showers. This feature is demonstrated in Fig.4 where a measured energy spectrum is shown for electromagnetic and hadronic showers for data taken in 1999. The large tail at high energy is due to the bad performance of the old FNC spaghetti calorimeter.

2.2 Main calorimeter

A new Main Calorimeter is a sandwich-type calorimeter consisting of four identical sections with transverse dimensions 600×600 mm² and 516 mm long. Each section consists of 25 lead absorber plates (4% Sb) 14 mm thick, and 25 active boards with 3 mm scintillators *Kuraray* SCSN-81. Each active board is made of 6 scintillating tiles with the transverse size of 198 mm \times 198 mm and two tiles with transverse size of 198 mm \times 258 mm (see Fig.5).

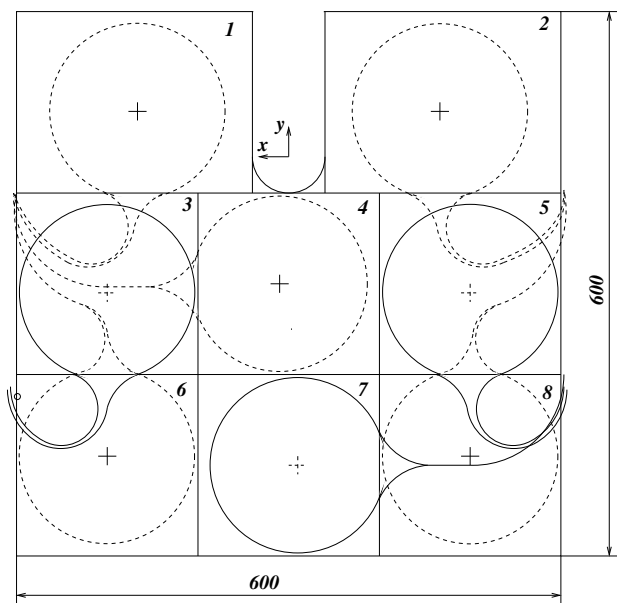


Figure 5: *Layout of tiles on active board and positions of readout and light guide fibres.*

The 25 tiles of one section with the same transverse position form a "tower". All together there are 32 towers in all four sections. In the top part of the calorimeter there is a special opening for the proton beam vacuum pipe which is going through the calorimeter as seen from Fig.1. The total length of the Main calorimeter is 2064 mm.

The light from each scintillating tile is collected by a 1 mm diameter Wave Length Shifter fibre (*Kuraray* WLS Y11-200M). It is located in the groove on the scintillator surface and through light connectors is attached to two 1 mm transparent

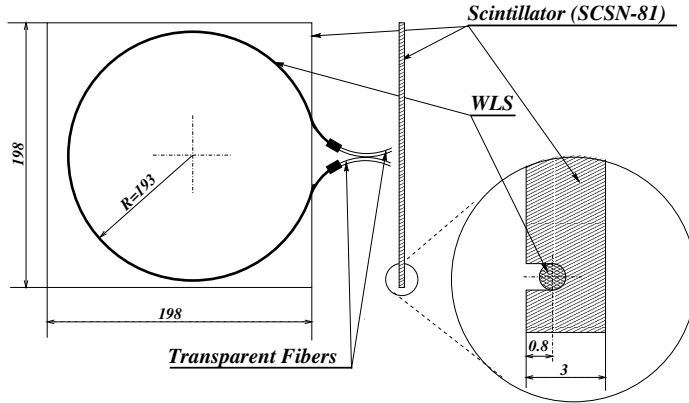


Figure 6: *Position of WLS in scintillator.*

PSM fibres (see Fig.6). 50 transparent fibres from one tower (2 fibres from each tile multiplied by 25 tiles in each tower) and one fibre from monitor light generator are assembled into one 51 fibres bundle and connected through 0.3 mm air gap to a center of photocathode of a *Philips XP2282B* photomultiplier tube (PMT). The 51-st fibre from a monitor light generator is used for an independent monitoring of the PMT gain (see below).

The Monte-Carlo simulation and radioactive source tests have been used to check the uniformity of the scintillator response. The results are shown in Fig.7, where each histogram corresponds to a scan of the scintillator along the horizontal line, as shown in the right bottom part of the figure. The worst uniformity is observed for the most upper line. The tests with the radioactive source and the Monte Carlo calculations give similar results.

The scintillators are wrapped up with the high reflection *Tyvek* paper 0.2 mm thick and are fastened between two 0.3 mm stainless steel plates. To provide an uniformity of assembling and to prevent the details of the active board from moving during a transportation a few thin (2 mm) *Rohacell* spacers are inserted and all details of active board are fixed using double *Scotch* tape. All absorber plates and active boards of one section are mounted on a stainless steel plate 10 mm thick and put into light tight aluminium box with the external dimensions 695 mm(width) \times 859 mm(height) \times 516 mm. In the upper part of the box there is a compartment \sim 170 mm high where PMT and monitor light generators are placed.

A light emitting diode (LED) monitoring system is foreseen to monitor the gain variation of the photomultipliers and the light yield of the scintillators. The light from blue LED is distributed by transparent fibres to each scintillator of every fifth active board. For this purpose two light generators are installed in the PMT compartment of each section. Each light generator works for four towers. Totally eight light generators are used. The system allows to monitor both the optical connections in the whole system and any radiation damage of the scintillators.

The gain of PMT is permanently monitored by another independent monitoring system. The light from one light generator with a blue LED is directly distributed over all PMT through transparent fibres. Each fibre is combined with other 50 signal fibres into the same bundle and this bundle is attached to photocathode of the PMT.

To control a stability of the light generator a special additional monitor PMT is

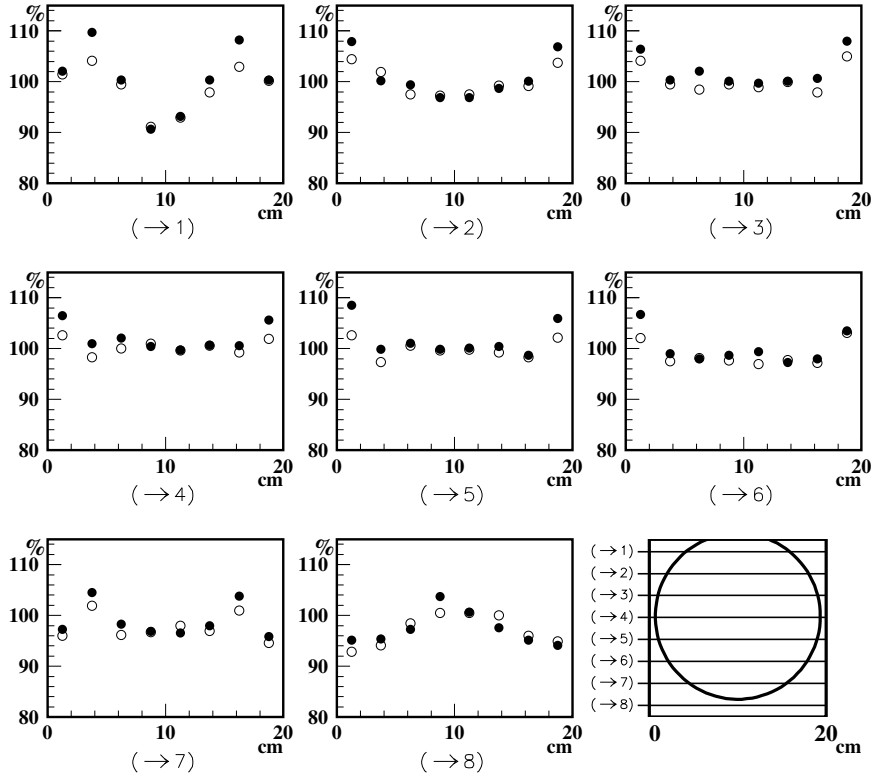


Figure 7: The result of scan of a scintillator with a radioactive source (black circles) and the Monte-Carlo simulation (open circles). 100% corresponds to read out in the center of the tile. The directions of the scans are shown in the right low part of the figure.

used. It is installed outside the calorimeter in a small light tight box and accepts the light both from the light generator through a transparent fibre and directly from a small piece of scintillator $20 \times 20 \times 2 \text{ mm}^3$, which is irradiated by alpha particles with energy 5.5 MeV from radioactive Am^{241} .

The signal and light distributions for one section are shown in the Fig.8. The monitor PMT and its light generator are common for all four sections of the FNC and are marked in the figure by a dotted line. The pulse generator drives the monitor light generator and the rest light generators alternately with odd and even pulses to distinguish the monitor signals during the analysis.

3 Beam tests

The new FNC has been tested at several places:

- 8 GeV proton beam at ITEP – operation tests, preliminary calibration;
- SPS beam (120–350 GeV) at CERN – final (absolute) calibration;
- DESY: Petra West and Hera North – Photomultiplier/Scintillator monitoring system development and tests;
- HERA beam at DESY: Tests of the FNC *in situ*.

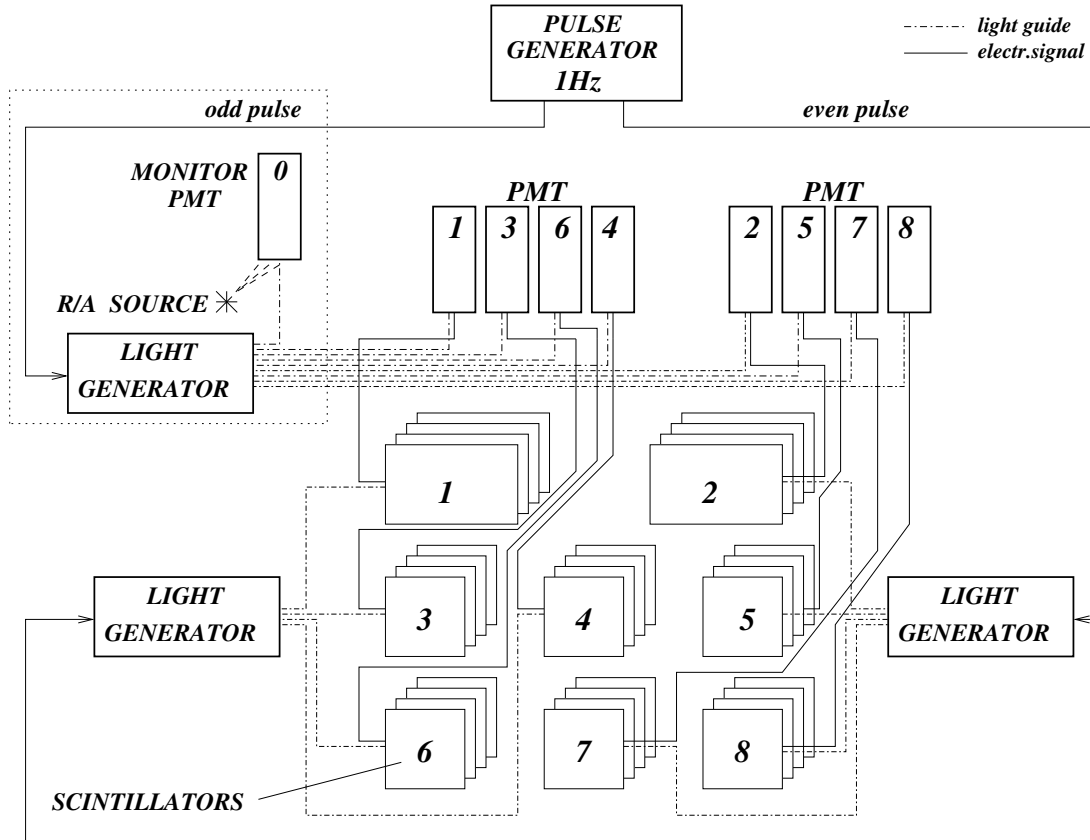


Figure 8: *Calorimeter monitoring. Only one section is shown. The monitor PMT, the light generator and the radioactive source are common for all four sections and marked by a dotted line.*

3.1 Tests at ITEP

Preliminary tests of the Main Calorimeter sections were done at ITEP Y-10 proton accelerator. The first three sections were tested separately at 8 GeV hadron beam. The sections were mounted on a moving table, so the coordinate scan was possible on the whole area of the section. For the beam formation five scintillating counters were used. Four counters were installed in front of the test section and one counter was installed behind the section to identify punch-through particles. The beam transverse cross section was about 1 cm^2 . For the readout LeCroy 1449A 0.25 pC/channel CAMAC ADC was used. A typical spectra is shown in Fig.9. The first peak at ~ 13 ADC counts is a pedestal, the second peak at ~ 25 ADC counts corresponds to MIP particles and the broad bump with mean value about 60 ADC counts corresponds to hadron showers.

In Fig.10 result of a horizontal scan at median line of one of the sections is shown. The scan was extended for three towers of the section. The readout signal is a sum of signals from all three towers. One can see the decrease of the section response at the edges of the section and decrease of the signal during the crossing of a tower

boundary.

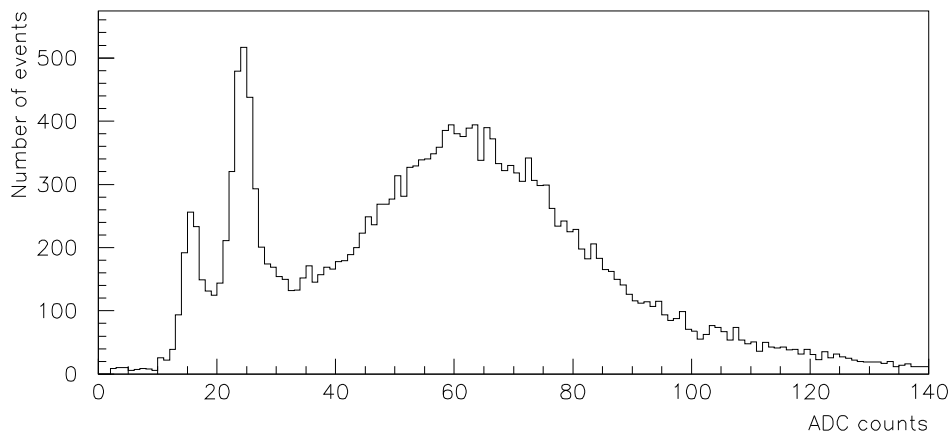


Figure 9: *Energy spectrum for 8 GeV beam during the ITEP tests. The first peak at ~ 13 ADC counts is a pedestal, the peak at ~ 25 ADC counts is a result of punch-through particles and the broad bump with mean value about 60 ADC counts corresponds to hadron showers.*

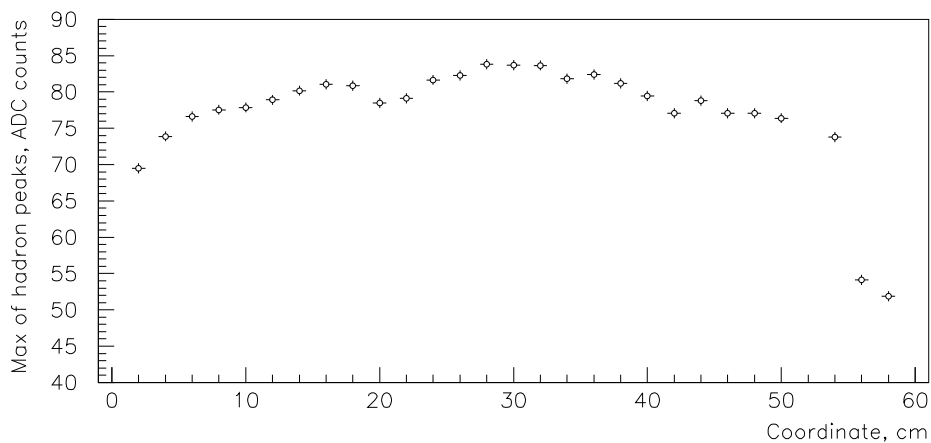


Figure 10: *Horizontal scan by 8 GeV beam.*

The visible asymmetry around the center of the section can be explained by non-zero impact angle ($\sim 2^\circ$). As it follows from the picture, the homogeneity of the section response in a central part of the section (± 20 cm) is not worse than $\pm 4\%$.

The ITEP test runs allowed to do a preliminary determination of HV for PMT and an initial calibration at 8 GeV.

3.2 Tests at CERN

Tests of the new FNC at CERN were done in SPS beam-test areas H6 (14-26 of June 2000) and H4 (13-16 of July 2000). In the H6 area positrons up to 150 GeV and pions/protons up to 180 GeV were available. In the H4 area electrons of up to 225 GeV and protons of up to 350 GeV were available. The basic procedure was to collect data with beams exposing the centers of towers of the Main Calorimeter or center of strips of the Preshower. Coordinate scans with 3 mm and 1 cm steps were also done for the determination of coordinate weighting functions.

3.2.1 Experimental setup

In both beam-test areas the whole FNC or the individual sections were installed on moveable platform. The scintillating counters 40×40 mm², 20×20 mm², 10×10 mm² and 3×3 mm² were used for trigger purpose, depending on the beam intensity and coordinate precision requirement. The trigger scintillators were installed from 2 m to 7 m distance upstream the FNC. For monitoring of photomultipliers gain LED light pulses from custom made pulse generators were used. Pulses were sent to the calorimeter at the 10 Hz rate.

3.2.2 Electronics

Light signals from 4×8 towers and 2×9 strips of calorimeter were fed into 50 Philips XP2282/B 8-stage photomultipliers. HV supply was one crate of LeCroy 1440 High Voltage System. Five 16-channel Struck F1002 VME FADCs were used as digitizers. The FADCs have 8-bit output data width, but dynamic range of input signal was artificially extended by nonlinear (hyperbolic) input network. Input range was 30 mV–350 mV and 60 mV–4.5 V depending on the type of preamplifier attached to the input of FADC channel. The least significant bit was 3 mV near 0 volt and 5 mV or 60 mV in the end of the scale. The FADCs were sampling at 94.65 MHz, what was defined by a custom made clock generator, while in nominal DESY conditions the nominal sampling rate is 104 MHz. The beam-test data were recorded as the plain digitized voltage versus the time sweep. The duration of sample was 40 points, which was equivalent to 420 ns in time.

3.2.3 Data collected

In the H6 area the following arrangements of the calorimeter components were used: Section 4; Section 3 and 4; Section 2, 3, and 4; Sections 1, 2, 3, and 4; and the full calorimeter setup – the Preshower in front of Sections 1, 2, 3, and 4. The beam was exposing the centers of the towers of each section and strips of the Preshower. In the H4 area, due to lack of the beam time, only the full calorimeter setup was scanned. Totally we have collected 17 million events.

4 Analysis of Results

The installation procedure of the FNC sections on moveable platform, described in 3.2.3, allowed to test and calibrate each FNC tower separately. First of all the SPS electron beam with energy 120 GeV was used for tuning of the PMT high voltage to equalize a response from all channels. The beam consecutively has hit the center of each tower and HV was tuned to get the response from each tower to be equal to 250 ± 5 pC.

The hadron beams (protons and pions) were used for the tests and calibration. A typical response of the calorimeter for different beam energies is shown in Fig.11. The total signal is a sum of signals from all channels of the Preshower and all channels of the Main calorimeter.

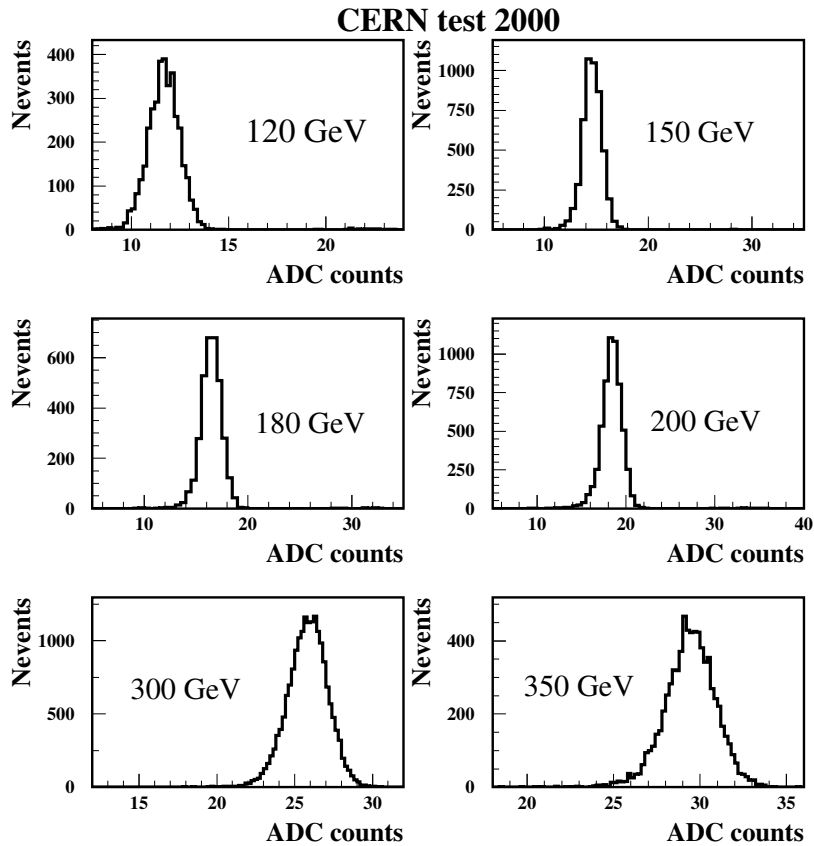


Figure 11: *FNC response at different hadron beam energies.*

The energy response of the calorimeter for electron and hadron beams as a function of beam energy is shown in Fig.12. The straight lines are linear fits. There are two comments to this picture. First, in spite of rather good linearity ($\lesssim 3\%$) the lines do not go to the origin of coordinate, especially for electrons. Second, the lines have different slopes and at high energy the e/p ratio is equal to 0.89 what is smaller than expected for almost compensated hadron calorimeter (we expected the e/p ratio about 0.94 according to MC simulation).

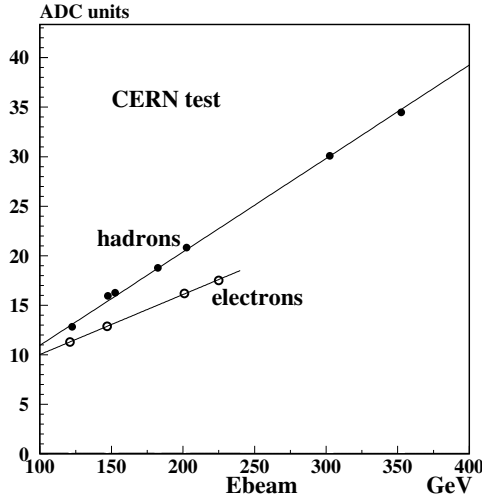


Figure 12: *Energy dependence of FNC for hadrons and electrons.*

The investigation of this phenomena has shown, that some characteristics of the calorimeter have nonlinear behavior. For example, a dependence of the energy deposited in the first section of the FNC (E_1) versus the sum of energies in the rest three sections E_{2+3+4} is not linear, as should be for a monochromatic beam (see Fig.13a). Responsible for this effect can be a nonlinearity of PMT which were used from the old FNC installation.

The understanding of non-linear effects in CERN test beam data is very important for the FNC because the beam energy at HERA (920 GeV) is much higher then the highest beam energy available at CERN (350 GeV); therefore, understanding of the response at low energies is needed for the extrapolation.

A systematic study of the PMT has been undertaken. For that purpose a special installation was designed and constructed at ITEP, which allowed to produce the different light beam independent of a possible nonlinearity of the LEDs. A bright blue LED, used as a primary source was fired by an external pulse generator. The light from LED was collected by four transparent fibres. Output ends of the fibres were fixed and form a matrix 2×2 . For a screening of the light a rotating disk with 16 different holes combination was used. Disk had 16 fixed position and in each position only one combination of the holes was fitted for the light passing. As result 16 different light flows could be applied to a PMT. Using single opening matrix all four light fibres could be independently calibrated. Additional neutral light filters were applied to extend the light flow range to low values.

The results of the measurements show that the light dependence of PMT outputs has a noticeable deviation of linearity. The reason for that is wrong HV which was applied to the last PMT dinodes. The design of HV divider for PMT has foreseen a special boost HV to feed last dinodes of PMT. Unfortunately this additional boost HV was not on during the CERN test. Our special measurements, which were done after CERN test, have shown that the linearity of the used PMT strongly depends on

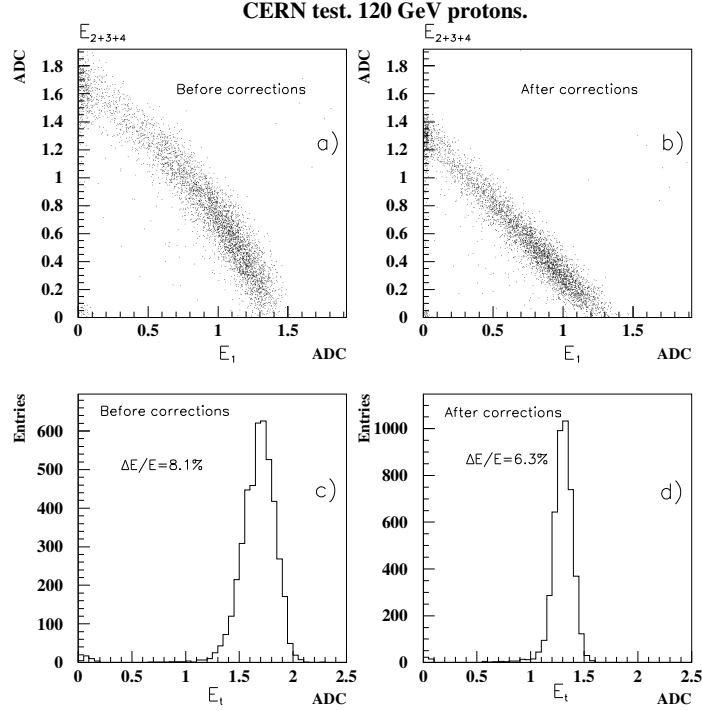


Figure 13: *CERN measurements at 91 GeV proton beam. E_1 is energy deposited in the first section, E_{2+3+4} is the sum of energies deposited in the rest three sections. The E_t is the sum of energies in all four sections. a) and c) before corrections, b) and d) after corrections for nonlinearity (see text).*

boost HV. In Fig.14 dependence of the output signal from the PMT on light input signal from just described above ITEP installation was shown for different boost HV. The boost HV is measured in percents from the main HV. With the boost HV about 30-35% from the main HV the deviation from linearity is not more than 1-3%, depending on a PMT sample. The dependence of a PMT response without the boost HV as function of the response with boost is shown in Fig.15 for different light intensity by circles, squares and triangles for two PMT and two different HV. In the same figure with black points the LED signals from all towers of the FNC are plotted. One can see that the reduction of signals without boost HV depends on the light signal only and almost does not depend on PMT and applied HV. The solid line is result of fitting black point by empirical function

$$S_{nb} = a \times \ln(1 + b \times S_b) \quad (1)$$

with two parameters $a = 323 \pm 2$ and $b = 0.0064 \pm 0.0001$. S_{nb} - signal without boost HV and S_b - signal with boost HV.

A similar study was done at DESY. At the DESY installation the fact of the PMT response linearity when HV boost is applied was used and dependence of the PMT output without HV boost as a function of the PMT output with the boost for

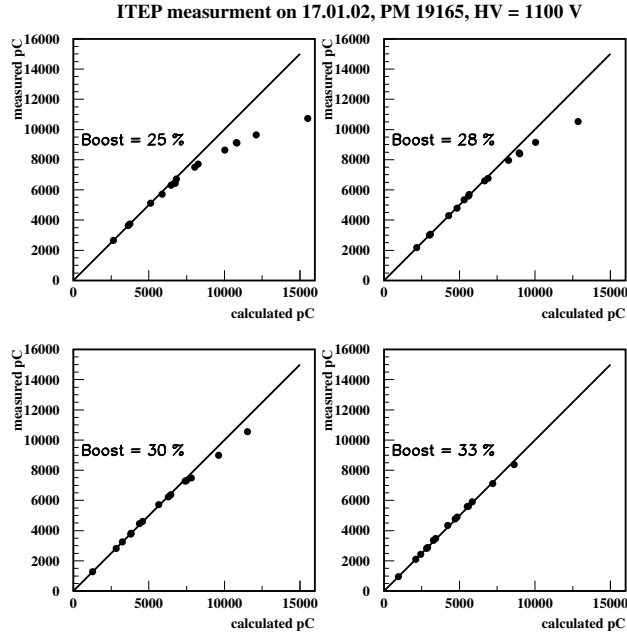


Figure 14: *The dependence of LED signal for different boost HV (measured relatively main HV) on calculated light signal in accordance with calibration.*

a few PMT was measured. The measurements show that in our working region all measured PMT have the similar nonlinearity without boost HV.

Using the correction factors based on the determined nonlinearity one can apply this corrections to our CERN data. The results can be demonstrated in Fig.13c, where the same dependence, as in Fig.13a, is shown after the corrections. This correction procedure improves also the energy resolution as one can see comparing Fig.13c (before the correction) and Fig.13d (after the correction).

In Fig.16 the corrected results for different beam energies is shown. The solid line is a result of fitting with equation:

$$\sigma_E/E = \sqrt{\frac{A^2}{E} + B^2} \quad (2)$$

The FADC used during the CERN test have one more additional factor which deteriorates resolution because of variable phase difference between a strobe signal and the data signal. Due to technical reason a synchronization of the signals could not be on during the CERN tests and the additional resolution lose was about 0.1%. Finally, taking into account this correction the resolution of the new FNC is equal to:

$$\sigma_E/E = \left(\frac{63.4 \pm 4.7}{\sqrt{E[GeV]}} \oplus (3.0 \pm 0.4) \right) \% \quad (3)$$

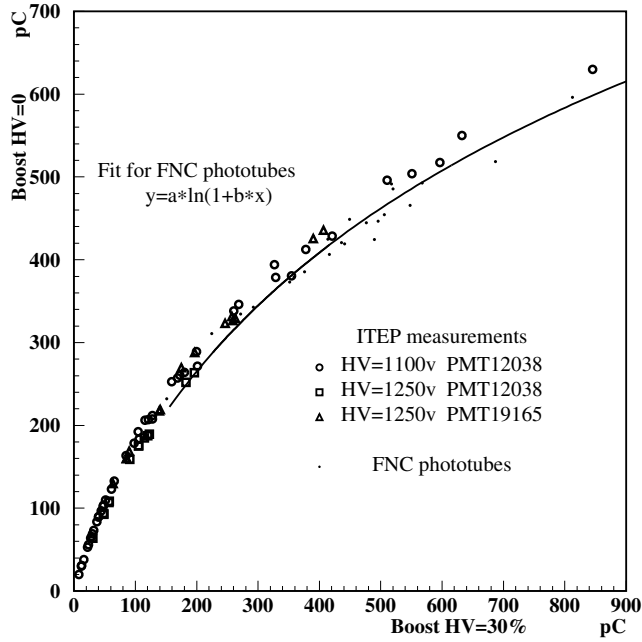


Figure 15: *The dependence of LED signal without boost HV on the same signal with the boost equal to 30% from total HV.*

Another method of the calibration, based on the energy conservation in an event was developed too. The method is described in the Appendix A and gives the results, which are consistent with the just described ones.

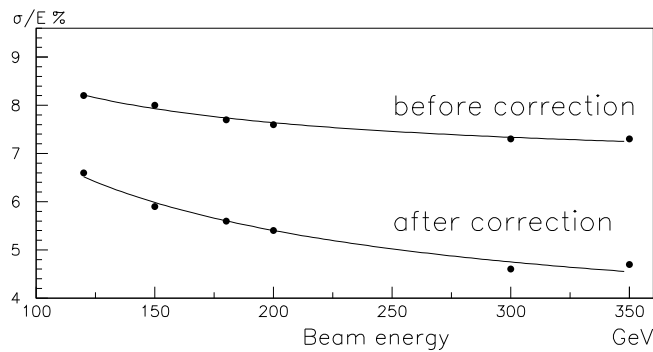


Figure 16: *The energy resolution of FNC from the CERN tests data before corrections for PMT nonlinearity and after the corrections.*

5 Comparison with MC

In this section a comparison of the CERN test beam results with Monte Carlo predictions obtained in framework of H1SIM simulation of FNC [7] is discussed.

The energy responses of the Preshower, the Main calorimeter and the complete FNC calorimeter at electromagnetic scale are shown in Fig.17 as a function of beam energy for the CERN test beam data and the H1FAST Monte Carlo used in H1 as a production MC. The H1FAST MC for the FNC was tuned [7] according to the response obtained from a simulation with FLUKA designed to describe the hadron-nucleus interactions at high energies and which well describes the main characteristics of hadronic calorimeters. As seen in Fig.17 the MC points are in good agreement with final results obtained in CERN tests.

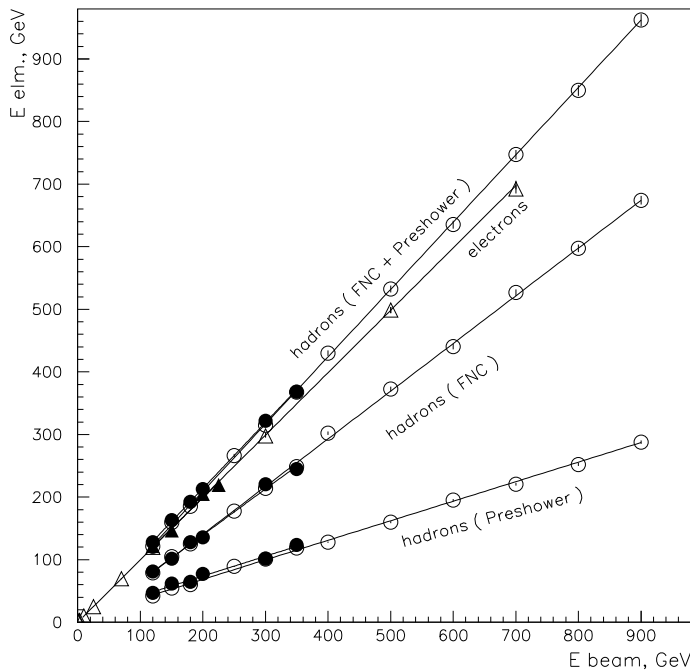


Figure 17: *The FNC energy response on electromagnetic scale including response in the Preshower and the Main calorimeter versus beam energy. The points: full circles - response to hadron beam from the CERN test, open circles - response to hadron beam from the H1FAST, full triangles - response to electron beam from the CERN test, open triangles - response to electron beam from the H1FAST.*

As already mentioned before (section 5) the e/π ratio for our type of hadron calorimeter should be about 0.94 in accordance with MC (FLUKA) calculations. However, the CERN test shows that without corrections the e/π ratio is much lower

than the predicted value and is energy dependent. After the correction for the PMT nonlinearity the CERN data are in good agreement with MC simulation (see Fig. 18).

The relative energy resolutions σ_E/E of the FNC obtained with high statistics of FLUKA calculations for hadrons of energies 350 GeV and 900 GeV are respectively: $(4.8 \pm 0.2)\%$ and $(3.9 \pm 0.2)\%$. This resolution is in good agreement with the CERN test results seen from Eq.(3).

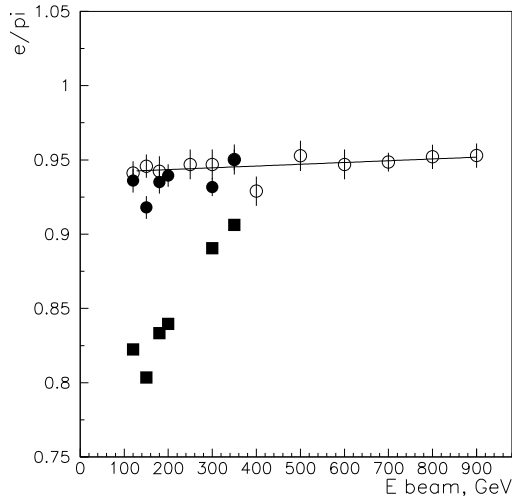


Figure 18: The e/π ratio versus beam energy for FLUKA MC (open points), CERN TESTs data before corrections (boxes) and after corrections (full circles).

6 FNC reconstruction program

The FNC reconstruction program – FNCREC is a part of H1REC package. The FNCREC reconstructs the energy and coordinates of particle detected in FNC. The program can be used both for the real data and for the MC simulation.

6.1 Reconstruction of electromagnetic scale energy

Input to FNCREC for real data is the raw bank LFNC which contains the digital samples of 52 readout channels (32 - Main Calorimeter, 18 - Preshower, 2 - Veto Counters). The digitized signals from LFNC bank are converted to the electromagnetic scale energies according to

$$E_i = C_i \cdot (L_i \cdot S_i), \quad (4)$$

where S_i are the digitized signals of single cells from LFNC bank, C_i are the calibration constants for conversion of FADC counts into GeV and L_i are the LED

correction factors defined as a ratio of current monitoring LED signal to the reference LED signal.

The reconstruction of electromagnetic scale energy for MC events is described in [7]. Reconstructed energies are stored in the ‘‘cell’’ FNCE bank. Finally, cells with energies greater than noise level are combined to reconstruct the clusters.

The next steps of reconstruction are the same for the real data and for MC. They can only differ by parameters used by reconstruction algorithms.

Since the small size of acceptance region and the transverse segmentation of FNC does not allow to make separation of clusters in multiparticle events, only one cluster in event is reconstructed and its reconstruction quality is given. All basic parameters of cluster, e.g. the cluster type, its energy, coordinates and other estimators are stored in the final output cluster bank FNCL. In the following a brief description of these parameters is given.

6.2 Cluster type

The cluster reconstruction begins with determination of Cluster Type based on shower energy distribution in the Preshower and the Main Calorimeter.

The Preshower provides the easy and efficient separation of electromagnetic and hadronic showers. Showers initiated by electromagnetic particles have fully deposited their energy inside the Preshower while hadronic showers have greater longitudinal development and as consequence, the significant energy deposition in the Main Calorimeter. The meaning of Cluster Type parameter is following: 1 - a cluster is fully contained in the Preshower (e.g. it corresponds to electromagnetic particle), 2 - a cluster is contained in the Main Calorimeter and 3 - a cluster has energy deposition both in the the Preshower and in the Main Calorimeter. The clusters with the Cluster Type equal to 2 or 3 correspond to hadrons.

6.3 Cluster energy

If energy is deposited in the Preshower only, then the electromagnetic shower is assumed and the cluster energy is determined as a sum of electromagnetic scale energies of all Preshower strips. In case of hadronic cluster the reconstructed energy is equal to sum of energies of all detector cells reduced to hadronic scale.

$$E_{cl} = \begin{cases} E_{elm}^P, & ClusterType = 1 \\ f(E_{elm}^P, E_{elm}^M) = E_{had}^P + E_{had}^M, & ClusterType = 2, 3 \end{cases} \quad (5)$$

where E_{elm}^P and E_{elm}^M are the electromagnetic scale energies of the Preshower and the Main Calorimeter correspondingly:

$$E_{elm}^P = \sum_{i=1}^9 Ex_i + \sum_{i=1}^9 Ey_i, \quad (6)$$

$$E_{elm}^M = \sum_{s=1}^4 \sum_{t=1}^8 E_{s,t}. \quad (7)$$

Here E_{x_i} and E_{y_i} are the energies in i -strip of X and Y projections correspondingly, and $E_{s,t}$ is the energy in t -tower of s -section of Main Calorimeter.

The hadronic energy for cluster of Type 2,3 is a sum of hadronic energies of the Preshower E_{had}^P and the Main Calorimeter E_{had}^M and is a function $f(E_{elm}^P, E_{elm}^M)$ of electromagnetic scale energies of the Preshower and the Main Calorimeter.

In MC simulation the relations between hadronic and electromagnetic deposited energies for the Preshower and the Main Calorimeter are known [7]. The functions which relate electromagnetic and hadronic scales were determined in CERN test data. The simplified expression to get hadronic scale for hadronic cluster is

$$E_{had}^P + E_{had}^M = C_1 \cdot E_{elm}^P + C_2 \cdot E_{elm}^M \quad (8)$$

with known C_1 and C_2 coefficients.

Finally, the hadronic scale energy for each cell is calculated according to the same proportion as electromagnetic energy contribution of cell to the electromagnetic energy in the full calorimeter. The corresponding variables of FNCE bank are filled.

6.4 Reconstruction of coordinates

Analysis of some algorithms for coordinates reconstruction in the Preshower and the Main calorimeter based on FNC simulation was performed in [7]. In this chapter the methods implemented in H1REC program are presented.

6.4.1 Preshower

The Preshower calorimeter provides high position resolution and in events with significant energy deposition in the Preshower the coordinates are determined by this subdetector.

Two methods of coordinate reconstruction are implemented. The choice of method is controlled by the corresponding parameter from so called Global Parameter's Table (FN1P) in NDB. The first method makes use of the fact that the shape of the Preshower energy response in five strips can be approximated by the falling exponential function and X-coordinate¹ of cluster can be defined as:

$$X_{rec} = X_i + C \cdot \ln \left(\frac{E_{i-1} + E_{i-2}}{E_{i+1} + E_{i+2}} \right) \quad (9)$$

where X_i is the coordinate of i strip with maximal energy E_i .

Another way to determine coordinates is to use the center of gravity (COG) method with linear weighting and to apply additional corrections:

$$X_{rec} = X_{cog} + C \cdot \sin \left(\frac{2\pi(X_{cog} - X_{center})}{l} \right), \quad (10)$$

¹For Y -coordinates the expressions are similar.

where X_{cog} is COG coordinate calculated with linear weighting, X_{center} is center of strip with maximal energy, and $l = 2.9$ cm is the width of the Preshower strips.

Both methods provide similar resolution, but the first one showed a better stability in critical cases and was chosen as default.

In general, the shape of the Preshower response depends on shower type (electromagnetic or hadronic) therefore the reconstruction program uses different constants C for different shower types.

6.4.2 Main Calorimeter

In $\sim 20\%$ of events the neutron passes through the Preshower without interaction and shower begins its evolution in the Main Calorimeter. Transverse segmentation of the Main Calorimeter does not allow to determine the coordinates with good precision, but it is still possible to evaluate the coordinates with precision better than 2 cm. Again two methods of coordinates reconstruction are implemented.

A method used as default is based on assumption that coordinates of the center of gravity calculated with the square root weighting have almost linear dependence on the real hit position inside the acceptance region. Taking into account that center of Main Calorimeter is shifted by X_{center} and correcting slope of dependence by dimensionless factor C , resulting formula can be written as:

$$X_{rec} = X_{center} + C \cdot (X_{cog} - X_{center}) \quad (11)$$

Another method is similar to the one used to determine coordinates in the Preshower:

$$X_{rec} = X_{cog} + C \cdot \sin\left(\frac{2\pi(X_{cog} - X_{center})}{L}\right) \quad (12)$$

where X_{cog} is COG coordinate calculated with linear weighting, X_{center} is center of central tower, $L = 20$ cm is the width of a tower.

6.5 Quality of reconstructed clusters

6.5.1 Quality definition

To define a quality of reconstructed cluster some additional estimators are foreseen. A special Quality word in the FNCL cluster bank is used, where bits are set to 1 if the cluster didn't pass the corresponding quality check.

- In case of a coincidence of the signals in both planes of the Veto Counter the incoming particle is considered to be charged and the first bit of the Quality word is set.
- **Core Energy** estimator is calculated as a ratio of energy deposited in the central towers to energy in whole Main Calorimeter:

$$CoreEne = \frac{\sum_{s=1}^4 E_{s,4}}{\sum_{s=1}^4 \sum_{t=1}^8 E_{s,t}} \quad (13)$$

The clusters initiated by particles with impact point inside acceptance region basically developed in the central towers. For such particles the Core Energy estimator assumed to be close to 1. If more then 50% of cluster energy is deposited in outer towers (that corresponds to $CorEne < 0.5$) then the second bit of the Quality word is set.

- If the Cluster Type is equal to 3 the coordinates of clusters can be calculated both in the Preshower and the Main Calorimeter. If the difference of this coordinates is too large ($> 6cm$) then it may mean that more than 1 particle hit the FNC, and the for this cluster the third bit of Quality word is set.

6.5.2 Other estimators

To provide the check of cluster quality the cluster radius $ECRA$ and second momenta $SecMom$ variables are implemented in the reconstruction program. The definition of cluster radius is

$$ECRA = \frac{\sum_{i=1}^N W_i \sqrt{(X_{cell,i} - X_{cl})^2 + (Y_{cell,i} - Y_{cl})^2}}{\sum_{i=1}^N W_i}, \quad (14)$$

where $X(Y)_{cell,i}$ and $X(Y)_{cl}$ are the coordinates of cell and cluster centers respectively, N is a total number of cells and W_i is the weight. Three variants of weight were considered:

$$W_i = \begin{cases} E_i, \\ constant + \ln(E_i), \\ \sqrt{|E_i|}, \end{cases} \quad (15)$$

The linear weighting allows better separation of electromagnetic and hadronic clusters. This conclusion was obtained from the MC by studying difficult for separation cases. The $W_i = E_i$ was chosen as a default in expressions (14) and (17).

The $SecMom$ variable with usual definition for second momenta can be used also for better selection and cross check of cluster quality.

$$SecMom = \sqrt{(\bar{X}^2 - \bar{X}^2) + (\bar{Y}^2 - \bar{Y}^2)}, \quad (16)$$

where \bar{X} , \bar{Y} are real coordinates of the cluster and

$$\bar{X}^2 = \frac{\sum_{i=1}^N W_i X_{cell,i}^2}{\sum_{i=1}^N W_i}, \quad (17)$$

6.6 Output banks

There are two banks at the reconstruction program output:

FNCE – FNC Cell’s bank, that contains for every FNC cell the deposited energy in electromagnetic and hadronic scales and time information of the signals.

FNCL – FNC Cluster bank, that contains the reconstructed cluster information.

Detailed description of these banks is given in Appendix B.

7 Tests at the HERA beam

The FNC was finally installed in the HERA tunnel in January of 2001. A few tests of the FNC *in situ* — linearity test and coordinate reconstruction test have been done.

In Fig.19 the cluster coordinate distribution is shown. It compares good both with a Monte Carlo simulation and with similar distribution from the previous years.

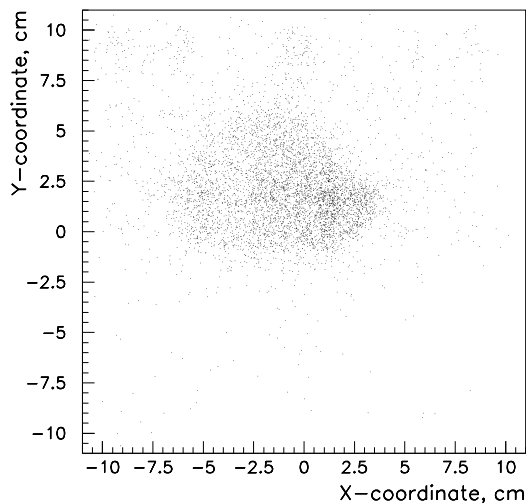


Figure 19: *FNC cluster center distribution for a beam-gas run.*

The linearity of the energy response of the FNC has been measured during dedicated energy rampings of the proton beam. For this purpose the proton beam which is injected at $E_p \sim 40$ GeV was not directly accelerated to its maximum energy of 920 GeV as usually, but instead it was kept at intermediate constant values allowing to measure the neutron energy spectrum obtained in beam-gas interactions at different nominal beam energies.

Since the shapes of the neutron spectrum are different for different beam energies we used the trailing edge of the spectrum rather than the peak position for the linearity measurement. The energy spectra and the dependence of the trailing edge of the FNC energy spectrum versus proton beam energy are shown in Fig.

20. Although the background conditions during these measurements were far from optimal, this result shows that the linearity is quite satisfactory.

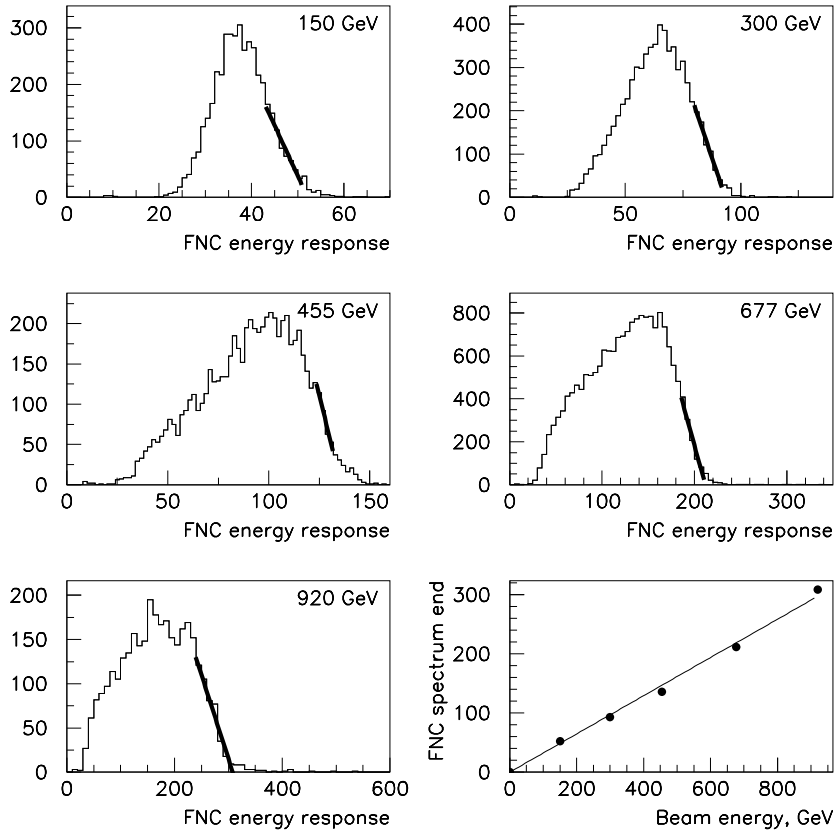


Figure 20: *Test of the FNC linearity. The spectra of the FNC energy response (given in units of ~ 3.2 GeV) are measured at different proton beam energies.*

8 Summary

The design parameters and the construction of a new H1 Forward Neutron Calorimeter (FNC) have been presented. The calorimeter was built and successfully installed during the shutdown 2000-2001. The on-line and off-line software for the new FNC has been developed and implemented. Test beam measurements as well as the experience of the first months of real data taking indicate that the design goals have essentially been reached. The energy response of calorimeter is linear up to 3% precision and the energy resolution is

$$\sigma_E/E = \left(\frac{63.4 \pm 4.7}{\sqrt{E[\text{GeV}]}} \oplus (3.0 \pm 0.4) \right) \%$$

References

- [1] “*Proposal for a Forward Neutron Calorimeter for the H1 Experiment at DESY.*” by W.Beck et al., August 1995
- [2] “*Measurement of Leading Proton and Neutron Production in Deep Inelastic Scattering at HERA.*”, by H1 Collaboration, *Eur. Phys. J. C* **6** (1999) 587.
- [3] “*Measurement of Dijet Production in Events with Leading Neutrons at HERA.*”, by H1 Collaboration, Contributed paper to Conferences EPS-2001 and LP-2001.
- [4] “*Online Detection of Neutrons With a Lead/Scintillating Fiber Calorimeter and a Scintillating Tile Hodoscope.*”, By M. Beck et al., *Nucl. Instrum. Methods A* **381** (1996) 330.
- [5] “*Upgrade of the H1 Forward Neutron Calorimeter.*” by W.Brückner et al., Internal note H1-11/99-578.
- [6] “*Performance of a Compensating Lead-Scintillator Hadronic Calorimeter.*” by E.Bernardi, *Nucl. Instrum. Methods A* **274** (1989) 134.
- [7] “*Different Aspects of the FNC Simulation in the Framework of H1SIM.*” by A.Zhokin, Internal note H1-07/2002-601.

APPENDIX A

A Check of FNC energy calibration

The method is presented to check the linearity of energy response in calorimeter with CERN test beam data. The method is based on the energy conservation in event. To reduce the number of free parameters the calibration procedure is fulfilled step by step: first - the calibration of FNC towers and then - the calibration of Preshower strips.

A.1 Description of calibration algorithm for FNC towers

To provide the check of energy calibration in every tower one should specify the value of energy in each bin of measured spectrum. At the beginning, to simplify the procedure, one can consider the case with one bin only i.e. one can find the correction factor to averaged value of energy deposited in a tower.

The energy contribution of one FNC tower i to energy in all towers N_{towers} averaged over all events N_{ev} can be characterized by the weight w_{0i} :

$$w_{0i}^n = \frac{1}{N_{ev}} \sum_{j=1}^{N_{ev}} \frac{f_i^n E_{ij}}{\sum_{i=1}^{N_{towers}} f_i^n E_{ij}}, \quad (18)$$

where f_i^n is the energy correction factors which can be applied to tower energy E_i on iteration n .

With the pull P_j^n defined in (20) below one writes the new weight w_1 of tower to be used for calculation of new correction factors:

$$w_{1i}^n = \frac{1}{N_{ev}} \sum_{j=1}^{N_{ev}} P_j^n \frac{f_i^n E_{ij}}{\sum_{i=1}^{N_{towers}} f_i^n E_{ij}} = \frac{1}{N_{ev}} \sum_{j=1}^{N_{ev}} \frac{E_{beam} f_i^n E_{ij}}{(\sum_{i=1}^{N_{towers}} f_i^n E_{ij})^2} \quad (19)$$

The pull:

$$P_j^n = \frac{E_{beam}}{\sum_{i=1}^{N_{towers}} f_i^n E_{ij}} \quad (20)$$

takes into account the energy conservation in event. With known weights defined in (18) and (19) the correction factors can be calculated for next iteration:

$$f_i^{n+1} = f_i^n \frac{w_{1i}^n}{w_{0i}^n} \quad (21)$$

The iterative procedure (18) - (21) is finished if the relative changes of correction coefficients becomes of order of few per mille:

$$\frac{f_i^{n+1} - f_i^n}{f_i^n} \sim 0.005, \quad (22)$$

Once iterative procedure is defined one can consider the common case to find corrections in each energy bin of every tower. One need to note that energy linearity of every tower can be checked only in the energy ranges available in CERN test beam data.

To define energy correction factors for i_0 tower the iterative procedure (18) - (22) has to be done for each energy bin k of chosen tower i_0 . The equations (18) - (22) will be changed according to:

$$\begin{cases} E_{ij} \longrightarrow E_{ijk} \\ f_i^n \longrightarrow f_{ik}^n \\ P_j^n \longrightarrow P_{jk}^n \\ w_i^n \longrightarrow w_{ik}^n \\ N_{ev} \longrightarrow N_k^{ev} \end{cases} \quad (23)$$

Note, that there is no attempt to specify simultaneously the correction factors for other towers in its own energy bins. Only one correction factor f_{ik}^n for tower i relating to k bin of tower i_0 is defining in iteration procedure. To some extent, this approach ignore the influence of possible non-linearity in energy in other towers, but reduce the number of free parameters to be specified and therefore improve the convergence of the procedure. To clarify more, one can write down the expression (21) in details:

$$f_{ik}^{n+1} = f_{ik}^n \frac{\sum_{j=1}^{N_k^{ev}} \frac{E_{beam} f_{ik}^n E_{ijk}}{(\sum_{i=1}^{N_{towers}} f_{ik}^n E_{ijk})^2}}{\sum_{j=1}^{N_k^{ev}} \frac{f_{ik}^n E_{ijk}}{\sum_{i=1}^{N_{towers}} f_{ik}^n E_{ijk}}} \quad (24)$$

A.2 Calibration of FNC towers

For calibration of FNC towers the CERN test data runs with hadron energy beam of 180 GeV were used. This energy was a maximal available beam energy in configuration of calorimeter without the Preshower. The final correction factors f_{ik}^{final} were obtained after four iterations in procedure (18)-(23).

The linearity can be seen as a dependence of the corrected energy $E_{corrected}$ versus measured energy $E_{measured}$, where

$$\begin{aligned} E_{corrected}(k) &= f_{i_0k}^{final} E_{i_0k}, \\ E_{measured}(k) &= E_{i_0k} \end{aligned} \quad (25)$$

Such a dependence for all FNC towers are presented in upper part of Figure 21. The measured energy is plotted in electromagnetic scale obtained from runs with 120 GeV electrons. The energy range is different for various towers. Only for three central towers where the largest portion of energy is deposited the energy ranges are maximal.

The corrected energy is plotted on absolute energy scale from equation (25), where the energy deposited in all towers is normalized to initial beam energy. The energy dependence shows the slight non-linearity for these three towers. Other towers which measure lower energies demonstrate linearity.

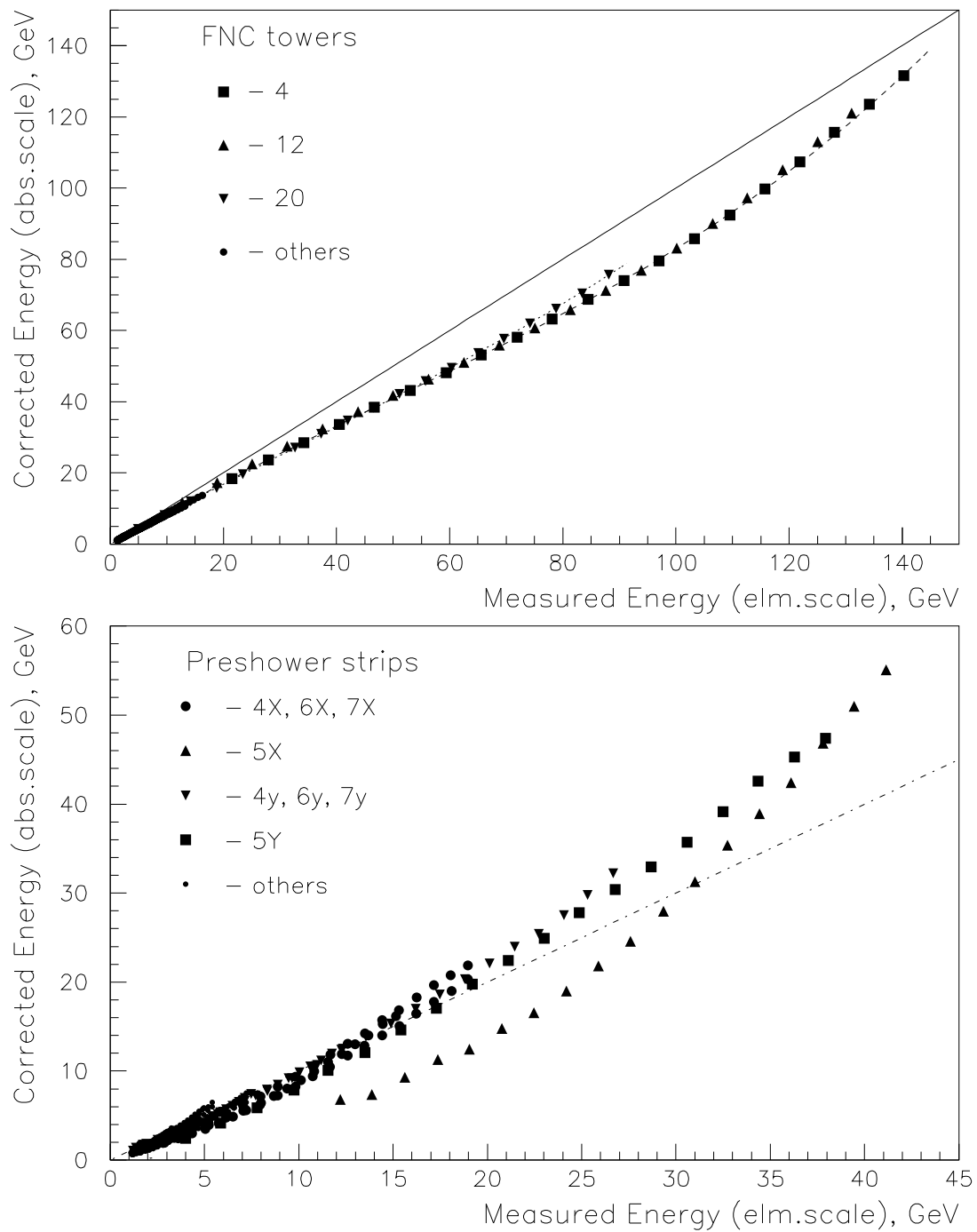


Figure 21: *The energy linearity for FNC towers and Preshower strips obtained with use of energy conservation in event.*

A.3 Description of calibration algorithm for preshower strips

With known energy contribution of all FNC towers one can consider similar algorithm for the Preshower strips. In the full calorimeter configuration with Preshower the absolute energy contribution of FNC main calorimeter is

$$E_j^{FNC} = \sum_{i=1}^{N_{towers}} f_i^{final} E_{ij} \quad (26)$$

The energy contribution of each preshower strip i to energy in full calorimeter is characterized by the weight w_{0i} :

$$w_{0i}^n = \frac{1}{N_{ev}} \sum_{j=1}^{N_{ev}} \frac{f_i^n E_{ij}}{(\sum_{i=1}^{N_{strips}} f_i^n E_{ij}) + E_j^{FNC}} \quad (27)$$

With the pull:

$$P_j^n = \frac{E_{beam}}{(\sum_{i=1}^{N_{strips}} f_i^n E_{ij}) + E_j^{FNC}} \quad (28)$$

one gets the strip weight w_{1i} specified by energy conservation:

$$w_{1i}^n = \frac{1}{N_{ev}} \sum_{j=1}^{N_{ev}} \frac{E_{beam} f_i^n E_{ij}}{((\sum_{i=1}^{N_{strips}} f_i^n E_{ij}) + E_j^{FNC})^2} \quad (29)$$

Then, the conditions (21) - (23) have to be applied.

A.4 Calibration of preshower strips

For calibration of Preshower strips the CERN test beam data runs with hadron energy beam of 350 GeV were used in full configuration of calorimeter. The final correction factors were obtained in iterative procedure (26) - (29), (21) - (23).

The linearity can be seen as a dependence of the corrected energy versus measured energy (see Eq. (25)) in the lower part of Figure 21. The measured energy is plotted on electromagnetic scale obtained from runs with 120 GeV electrons. The corrected energy is plotted on absolute energy scale from Eq. (28), where the energy deposited in all strips and FNC main calorimeter normalized to initial beam energy.

The energy range is different for different strips but is sufficient to see the slight non-linearity of energy calibration.

A.5 Some results with new calibration

To see what is achieved with the new energy calibration for all strips and towers of calorimeter the correlations of deposited energy with and without corrections were compared.

The correlations of measured energy are shown in Figure 22 for hadron beam energy 350 GeV. Upper plot presents the correlation of total energy E_{total} in full calorimeter versus energy E_{FNC} in main FNC calorimeter, lower plot– E_{total} versus energy in preshower $E_{preshower}$. The correlations of measured, non-corrected energy on electromagnetic scale are shown by circles. The correlations of measured, corrected energy on absolute scale are shown by squares. The correlations are significantly improved after energy corrections. The corrections were obtained as a result of polynomial description of calibrated points (see Figure 21). In the regions of extrapolation the polynomial curve can have the disagreement with real behavior of calibration. Because of this a slight deviation from straight line is seen in Figure 22.

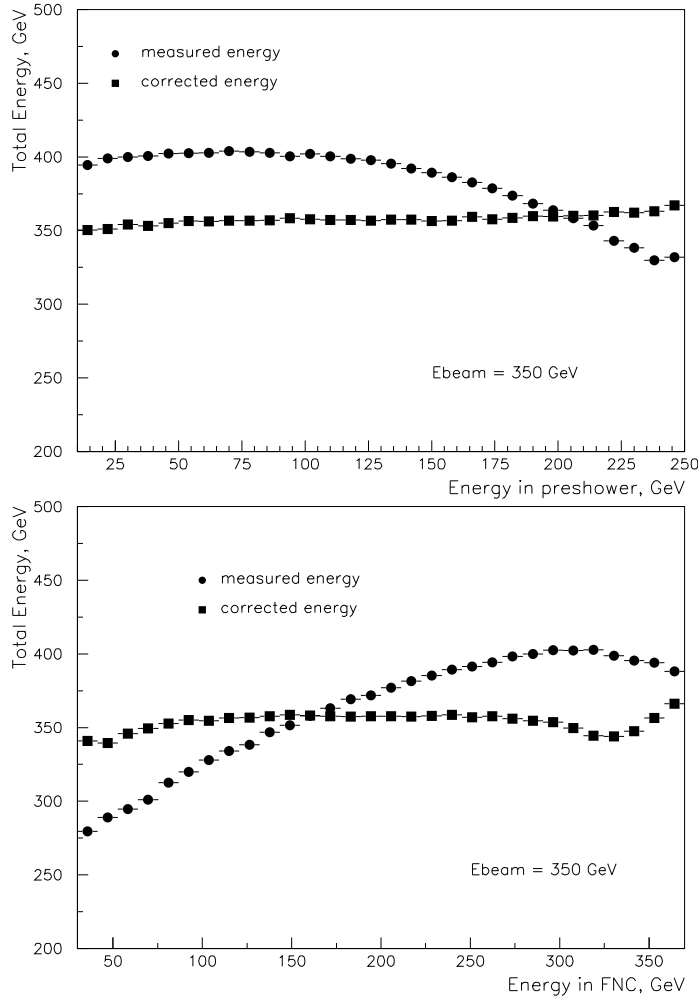


Figure 22: *Correlation of energy in full FNC calorimeter for hadron beam energy 350 GeV.*

Upper plot: the energy in full FNC calorimeter versus energy in the Preshower.

Lower plot: the energy in full FNC calorimeter versus energy in the Main calorimeter.

APPENDIX B

Bank FNCL - FNC Cluster Bank

Col	Name	Format	Min	Max	Comments
1	ClType	I	1	3	FNC Cluster Type 1 - electromagnetic (Preshower only) 2 - hadronic type 1 (MainCalo only) 3 - hadronic type 2 (Preshower+MainCalo) There is a signal if the sum of the energy over all cells (in elm. scale and with noise cuts applied) exceeds certain value (4. GeV for Preshower and 10 GeV for MainCalo)
2	Ecl	F	0.0	+inf	Cluster energy (final scale) [GeV]
3	Xcl	F			X coordinate of cluster
4	Ycl	F			Y coordinate of cluster
5	Zcl	F			Z coordinate of cluster
6	TimeToF	F	0.0	+inf	Not used
7	TimeCell	F	0.0	+inf	Time of the cell with maximal energy
8	ECRA	F	0.0	+inf	Estimator 1: Cluster R adius
9	CorEne	F	0.0	1.0	Estimator 2: Core Energy (E_4/E_{tot})
10	SecMom	F	0.0		Estimator 3: Second Momenta
11	Est4	F	-inf	+inf	Estimator 4: Energy in MainCalo
12	Quality	I	0	7	Cluster quality. See explanation in text
13	CaloCell	I			Towers which were used to compose cluster (for MainCalo)
14	PreshCell	I			Strips which were used to compose cluster (for Preshower)

Bank FNCE - FNC Cell Bank

The number of rows is exactly 52, where the row number corresponds to
1-32 - Main Calorimeter: 1-8 – section I, 9-16 – section II, 17-24 – section III,
25-32 – section IV
33-50 – Preshower: 33-41 – X strips, 42-50 – Y strips
51-52 – FNC Veto Counters

Col	Name	Format	Min	Max	Comments
1	Eelm	F	-inf	+inf	Cell energy at elm. scale [GeV] ([Volts] in case of Veto Counters)
2	Ehad	F	-inf	+inf	Cell energy at had. scale [GeV] (=Eelm in case of Veto Counters)
3	Time	F	-inf	+inf	Cell time (in ns)